



**HAL**  
open science

# Gesture Recognition Using Chipless RFID Tag Held in Hand

Zeshan Ali, Nicolas Barbot, Etienne Perret

► **To cite this version:**

Zeshan Ali, Nicolas Barbot, Etienne Perret. Gesture Recognition Using Chipless RFID Tag Held in Hand. 2022 IEEE/MTT-S International Microwave Symposium - IMS 2022, Jun 2022, Denver, Colorado, United States. hal-03765770

**HAL Id: hal-03765770**

**<https://hal.univ-grenoble-alpes.fr/hal-03765770>**

Submitted on 31 Aug 2022

**HAL** is a multi-disciplinary open access archive for the deposit and dissemination of scientific research documents, whether they are published or not. The documents may come from teaching and research institutions in France or abroad, or from public or private research centers.

L'archive ouverte pluridisciplinaire **HAL**, est destinée au dépôt et à la diffusion de documents scientifiques de niveau recherche, publiés ou non, émanant des établissements d'enseignement et de recherche français ou étrangers, des laboratoires publics ou privés.

# Gesture Recognition Using Chipless RFID Tag Held in Hand

Zeshan Ali<sup>#1</sup>, Nicolas Barbot<sup>#2</sup>, and Etienne Perret<sup>##3</sup>

<sup>#</sup>Univ. Grenoble Alpes, Grenoble INP, LCIS, 26000 Valence, France

<sup>\*</sup>Institut Universitaire de France, 75005 Paris, France

<sup>1</sup>zeshan.ali@lcis.grenoble-inp.fr, <sup>2</sup>nicolas.barbot@lcis.grenoble-inp.fr, <sup>3</sup>etienne.perret@lcis.grenoble-inp.fr

**Abstract**— In this paper, hand gesture recognition is presented by exploiting 3D localization using a depolarizing chipless RF identification (RFID) tag held in hand in front of a monostatic radar. The chipless RFID tag is localized by utilizing the backscattered phase and multilateration. Based on the location of the tag in 3D, it is possible to detect different gestures made with the hand. Six simple gestures are presented to illustrate the principle. These hand gestures are recognized by doing the free space measurements in office environment: a)  $x$  line; b)  $y$  line; c)  $z$  line; d)  $xy$  circle; e)  $xz$  circle; and f)  $xyz$  helix. The system is capable to recognize hand gestures with good accuracy and hand speed.

**Keywords**— chipless RFID, cross-polarization, depolarizing, radar cross section, radar scattering, radar polarimetry.

## I. INTRODUCTION

Hand gesture recognition is essential for human computer interaction. The main applications are gaming, sign language, virtual manipulation, daily assistance, palm verification, and human robot interaction [1]. These commercial applications have encouraged seeking new methods of gesture recognition. Some examples of hand gestures are pictographic gestures, kinetographic gestures, metaphoric gestures, and deictics as discussed in [2, Fig. 6]. Many sensors have been utilized for data acquisition: optical [3], acoustic [4], inertial [5], pressure [6], and radiofrequency (RF) [7]–[9]. Here, the acoustic, inertial, and pressure sensors are mostly active devices.

Chipless RF identification (RFID) presents many applications in the internet of things (IoT) and e-society: wireless identification [10], sensing [11], authentication [12], localization [13], and gesture recognition [8], [9]. The potential of chipless RFID based gesture recognition has been introduced in [8]. Likewise, a textile chipless RFID tag is presented in [9] for hand gesture recognition. This chipless RFID is constituted of a microstrip line (on the palm of the textile glove) and disconnected open stubs (on the fingers of the textile glove). These open stubs can be connected to the microstrip line by bending the finger. On the other hand, a chipless 2D localization and positioning technique is presented in [13].

In this paper, we are presenting a hand gesture recognition technique based on 3D localization of a chipless RFID tag held in hand. Here, 3D localization is different from 2D localization presented in [13]. The proposed technique is based on the phase information of the backscattered signal from the chipless RFID tag and the multilateration algorithm, where the 2D localization is extended to 3D localization without requiring a complex phase unwrapping procedure. Thus, this approach allows real time implementation and will be described in the following.

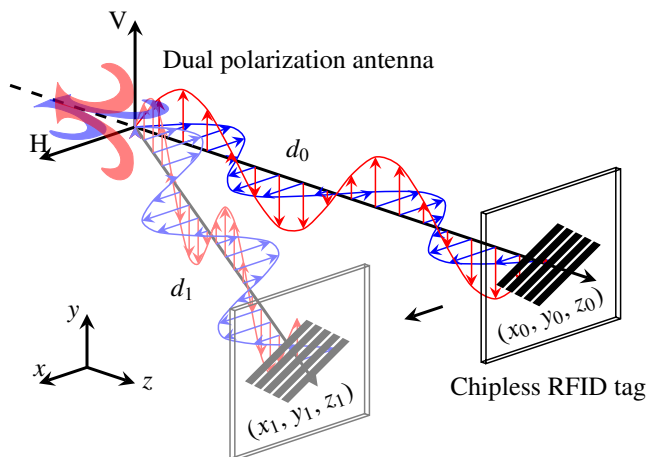


Fig. 1. Principle of operation of the proposed gesture recognition using a chipless RFID tag in front of the dual-polarization antenna. To simplify the representation, the chipless RFID tag is composed of a single resonator.

Owing to this proposed approach various hand gestures can be recognized: pictographic gestures, kinetographic gestures, and metaphoric gestures. Conversely, the hand gesture recognition method in [9] can merely recognize the finger bending gestures.

The proposed hand gesture recognition is a model based technique as compared to black box artificial intelligence methods (e.g., machine learning, deep learning, and neural networks) used by most of the visual sensors based hand gesture recognition techniques [3]. Furthermore, the presence of a chipless RFID label in gesture recognition makes the proposed technique suitable for other chipless RFID applications (i.e., identification, sensing, and authentication) in comparison to the Google Soli project [7].

The organization of this paper is as follows. Section II presents the mathematical model and chipless RFID design. Section III presents the measurements and gesture recognition. Section IV concludes this paper.

## II. MATHEMATICAL MODEL AND CHIPLESS RFID TAG DESIGN

The proposed gesture recognition requires a depolarizing chipless RFID tag in front of a single dual-polarization antenna with vertical  $V$  and horizontal  $H$  polarizations as shown in Fig. 1. The chipless RFID tag exhibits an initial 3D position  $(x_0, y_0, z_0)$  and the antenna to tag distance  $d_0$ . When the chipless RFID tag is moved to an unknown 3D position  $(x_1, y_1, z_1)$

and the unknown antenna to tag distance  $d_1$ , the displacement  $\Delta d$  can be estimated as (see [13] for 2D localization)

$$\Delta d = d_1 - d_0 = -\frac{1}{2k} \arg \left( \frac{M_{VH}^{d_1}}{M_{VH}^{d_0}} \right) \quad (1)$$

where  $k = 2\pi/\lambda$ ,  $M_{VH}^{d_0} = S_{VH}^{d_0} - I_{VH}$ ,  $M_{VH}^{d_1} = S_{VH}^{d_1} - I_{VH}$ .  $S_{VH}^{d_0}$ ,  $S_{VH}^{d_1}$ , and  $I_{VH}$  correspond to the cross polarization measured signal of the chipless RFID tag at  $d_0$ , the cross polarization measured signal of the chipless RFID tag at  $d_1$ , the cross polarization measured signal in the absence of chipless RFID tag (clutter), respectively.

It is important to note that in [13], the model (1) is solved in 2D (i.e., the tag is bounded in a given  $xy$  plane) and the phase  $\arg(M_{VH}^{d_1}/M_{VH}^{d_0})$  in (1) is unwrapped by a 2D phase unwrapping algorithm [14]. Here, the model (1) is solved in 3D (i.e., the tag is not bounded in a given  $xy$  plane) without using any 3D phase unwrapping method. Instead, the phase  $\arg(M_{VH}^{d_1}/M_{VH}^{d_0})$  in (1) is unwrapped on the occurrence of each phase shift of  $2\pi$  radians on a 3D gesture trajectory.

Multilateration is a well-known approach to locate a target, where the positions of at least three antennas are required (i.e., trilateration). In our case, multilateration is inverted such that having one antenna  $A$  and five scatterers as presented in Fig. 2. Note that in theory, three scatterers can be enough, but in practice to improve accuracy, five scatterers are used in this study. The initial distance  $d_0^{(i)}$  for each  $i$ th scatterer is supposed known. Furthermore, the relative distance among the scatterers is also known from the design of chipless RFID tag. Therefore from (1), the unknown 3D position  $(x_1, y_1, z_1)$  of the chipless RFID tag can be estimated by the multilateration algorithm [Fig. 2(a)] (see [13] for 2D localization).

The design of the proposed chipless RFID tag is based on five microstrip coupled dipoles tilted at  $45^\circ$  as shown in Fig. 2(b). The scatterers are realized on Rogers RO4003C substrate (dielectric permittivity  $\epsilon_r = 3.55$  and substrate height  $h = 0.81$  mm). The five scatterers are arranged in a check pattern on a Styrofoam to make the multilateration algorithm possible. The overall size of the proposed tag is  $9 \times 9$  cm<sup>2</sup>. For an in-depth discussion on the bandwidths and RCS levels of the microstrip coupled dipoles tilted at  $45^\circ$ , the reader is referred to [15, Chap. 4].

### III. MEASUREMENTS AND GESTURE RECOGNITION

The experimental measurements are done in an office environment with the depolarization chipless RFID [see Fig. 2(b)] held in hand in front of the monostatic radar with an antenna to tag distance of at least  $z = 10$  cm as shown in Fig. 3. The monostatic radar is set up by connecting the ports 1 and 2 of Agilent N5222 vector network analyzer (VNA) to V and H ports of Satimo QH800 dual-polarization horn antenna (0.8 – 12 GHz), respectively. The VNA output source power is -5 dBm. The measured parameter is the transmission coefficient (cross polarization). The data acquisition and postprocessing are done using a PC connected to VNA.

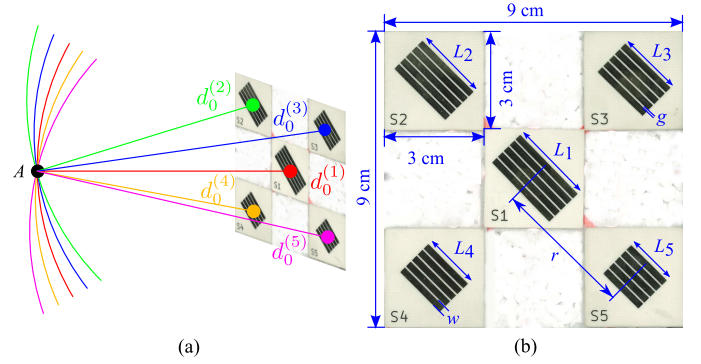


Fig. 2. (a) Principle of multilateration. (b) Photograph of chipless RFID Tag. The lengths of multiple coupled dipoles are  $L_1 = 24.8$  mm,  $L_2 = 21.8$  mm,  $L_3 = 19$  mm,  $L_4 = 16.8$  mm, and  $L_5 = 15$  mm. The microstrip trace width  $w = 2$  mm, the gap among microstrip dipoles  $g = 0.5$  mm, and the distance of off-centered scatterers from the origin  $r = 4.24$  cm.

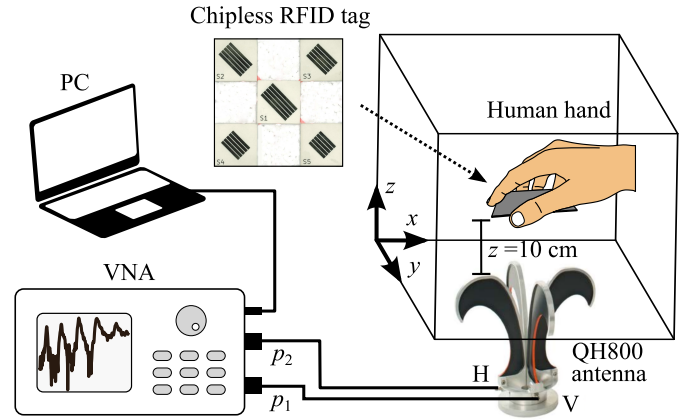


Fig. 3. Layout of the measurement setup.

Fig. 4 presents the calibrated measured cross polarization signals of the chipless RFID tag  $M_{VH}^{10\text{ cm}}$  and  $M_{VH}^{20\text{ cm}}$  in the line of sight of the antenna at  $z = 10$  cm and  $z = 20$  cm. From the magnitude responses in Fig. 4(a), five peak apexes associated with the resonance frequencies are observed in UWB: 3.19 GHz, 3.61 GHz, 4.11 GHz, 4.61 GHz, and 5.14 GHz. From  $z = 10$  cm to  $z = 20$  cm, the shifts in the phase can be observed in Fig. 4(b) (see at blue dashed lines). The phase information is extracted at each peak apex and then utilized in (1) to estimate the displacement  $\Delta d^{(i)}$  for each  $i$ th scatterer. Finally, the multilateration algorithm is applied [see discussion for Fig. 2(a)] to localize chipless RFID tag in 3D.

In Fig. 4, the frequency is swept from 3 to 5.5 GHz with 1001 points which takes a sweep time equal to 7.27 ms. For real time implementation of gesture recognition using chipless RFID tag, fast data acquisition is needed. For this purpose, the frequency is swept merely for five points related to the peak apexes, allowing to reduce the sweep time to 36  $\mu$ s.

Six ideal trajectories for various hand gestures are depicted in Fig. 5: a)  $x$  line; b)  $y$  line; c)  $z$  line; d)  $xy$  circle; e)  $xz$  circle; and f)  $xyz$  helix. These gesture trajectories are then drawn real time by a human hand holding the chipless RFID tag in front of the antenna of the monostatic radar system (see

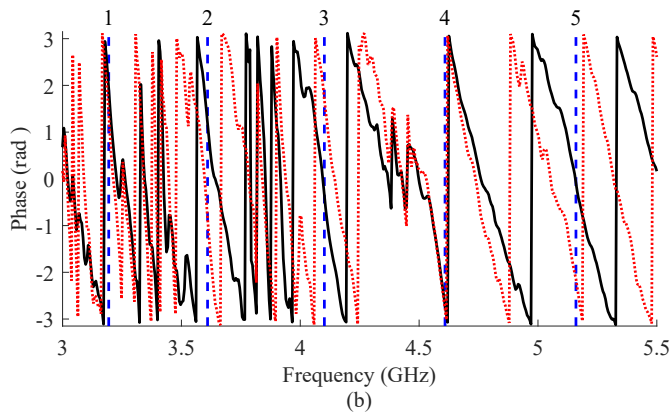
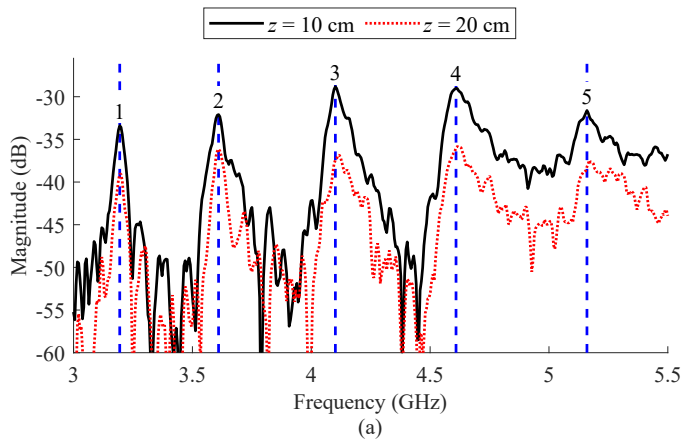


Fig. 4. Measured cross polarization signals of chipless RFID tag in the line of sight of the antenna at  $z = 10$  cm and  $z = 20$  cm. (a) Magnitude responses. (b) Phase responses.

Fig. 3). Fig. 6 presents the estimated hand gestures by using the chipless RFID tag held in hand. Fig. 6(a) to Fig. 6(c) present the estimation of the straight  $x$ ,  $y$ , and  $z$  lines (2D), respectively. Fig. 6(d) and Fig. 6(e) present the estimated  $xy$  and  $xz$  circles (2D), respectively. Finally, Fig. 6(f) presents the estimated  $xyz$  helix (3D). It can be observed that the gestures are well detectable. The proposed technique is capable to detect curved trajectories in 3D. The inaccuracies in the trajectories are mainly due to human error. However, 3D localization with very high precision is not needed for the gesture recognition application.

A video demonstration of the hand gesture recognition using the chipless RFID tag held in hand is uploaded online [16] (click on the link to watch the video). First, a labeled view of the chipless RFID measurement setup is shown. Then, real time hand gestures and their estimations are presented. From the video, it can be observed that as the human hand is introduced to hold the chipless RFID tag, the estimated position (see red point) gets disturbed (due to the direct reflections from the human hand) and becomes stable after a few instants. It shows that the human hand presents a negligible effect on the accuracy of the system. Owing to the fast acquisition from VNA and ordinary processing of a PC, the proposed method is capable to recognize the hand gestures at nominal speed.

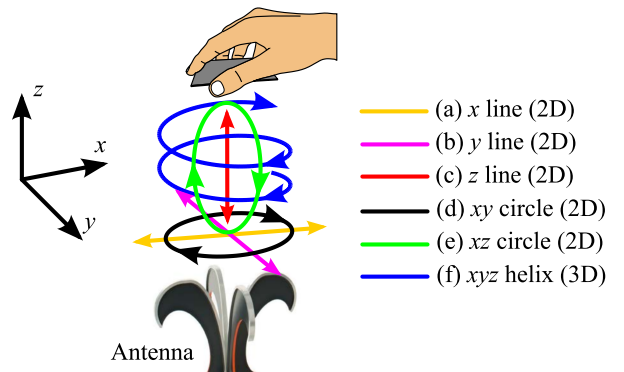


Fig. 5. Illustration of the six ideal trajectories for various hand gestures.

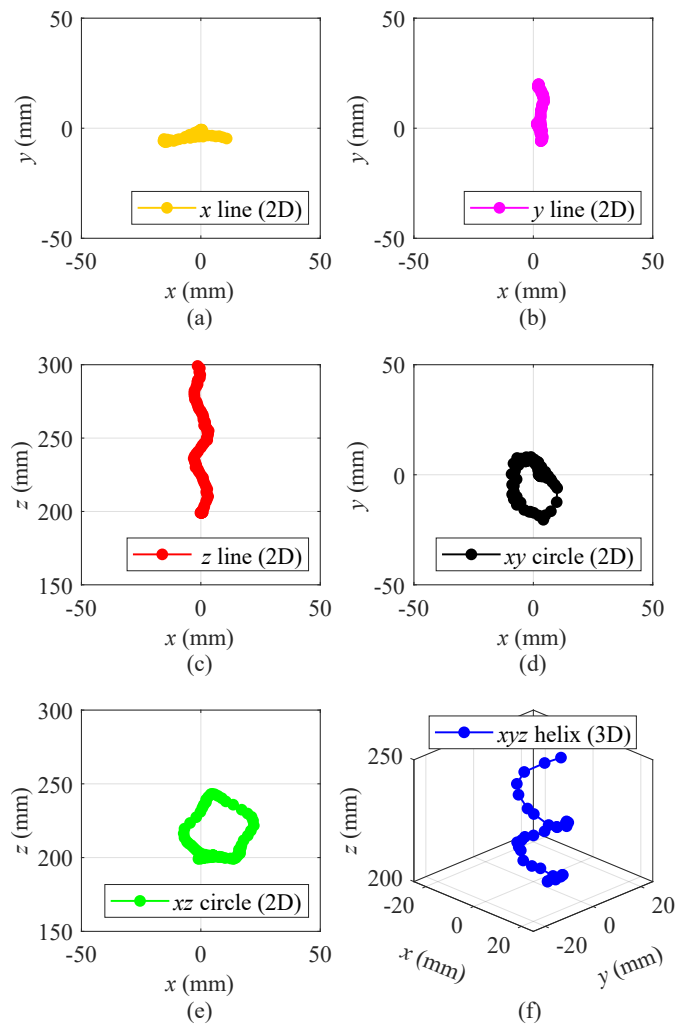


Fig. 6. Estimated hand gestures based on measurement results. (a)  $x$  line. (b)  $y$  line. (c)  $z$  line. (d)  $xy$  circle. (e)  $xz$  circle. (f)  $xyz$  helix.

The proposed method presents significant possible applications, for example, 3D computer mouse. In this case, it is possible to use displacements in  $xy$  plane to move the cursor and to use gestures like  $z$  line or  $xz$  circle for user click on the buttons present on a classical mouse.

#### IV. CONCLUSION

Gesture recognition as a novel application of the chipless RFID system was presented in this work. This capability was achieved by 3D localization of the chipless RFID tag. The design of the employed chipless RFID tag was constituted of five depolarization scatterers arranged in a check pattern to implement the multilateration algorithm for 3D localization. Six gesture trajectories drawn by a human hand holding a chipless RFID tag were recognized. Insofar as the method is based on an analytical approach allowing the localization of the tag, there is no limitation on the number of potentially detectable gestures. Also, this method is compatible with all the functionalities of chipless tags, such as the possibility of identifying the individual who seeks to interact with the reader. A real time video of operation was uploaded online [16] and it was observed that the human hand presents minimal effect on the accuracy of the gesture recognition system.

#### ACKNOWLEDGMENT

This work is funded by the European Research Council (ERC) under the European Union's Horizon 2020 research and innovation program under grant agreement no. 772539 (SCATTERERID, <https://www.scattererid.eu/>). The authors are thankful to Ms. Nathalie Franck for her help in proofreading this paper.

#### REFERENCES

- [1] H. Cheng, L. Yang, and Z. Liu, "Survey on 3D Hand Gesture Recognition," *IEEE Trans. Circuits Syst. Video Technol.*, vol. 26, no. 9, pp. 1659–1673, Sep. 2016.
- [2] Yanghee Nam, Nwngyun Wohn, and Hyung Lee-Kwang, "Modeling and recognition of hand gesture using colored Petri nets," *IEEE Trans. Syst., Man, Cybern. A, Syst., Humans*, vol. 29, no. 5, pp. 514–521, Sep. 1999.
- [3] M. Al-Hammadi *et al.*, "Deep Learning-Based Approach for Sign Language Gesture Recognition With Efficient Hand Gesture Representation," *IEEE Access*, vol. 8, pp. 192 527–192 542, 2020.
- [4] N. Siddiqui and R. H. M. Chan, "Hand Gesture Recognition Using Multiple Acoustic Measurements at Wrist," *IEEE Transactions on Human-Machine Systems*, vol. 51, no. 1, pp. 56–62, Feb. 2021.
- [5] Y. Liu, Y. Zhang, and M. Zeng, "Novel Algorithm for Hand Gesture Recognition Utilizing a Wrist-Worn Inertial Sensor," *IEEE Sensors J.*, vol. 18, no. 24, pp. 10 085–10 095, Dec. 2018.
- [6] P. B. Shull, S. Jiang, Y. Zhu, and X. Zhu, "Hand Gesture Recognition and Finger Angle Estimation via Wrist-Worn Modified Barometric Pressure Sensing," *IEEE Trans. Neural Syst. Rehabil. Eng.*, vol. 27, no. 4, pp. 724–732, Apr. 2019.
- [7] J. Lien *et al.*, "Soli: Ubiquitous Gesture Sensing with Millimeter Wave Radar," *ACM Trans. Graph.*, vol. 35, no. 4, Jul. 2016.
- [8] N. Barbot and E. Perret, "Gesture recognition with the chipless RFID technology," in *32nd Gen. Assem. Sci. Symp. Int. Union Radio Sci. (URSI GASS)*, Montreal, QC, Canada, Aug. 2017, pp. 1–3.
- [9] G. Monti, G. Porcino, and L. Tarricone, "Textile Chipless Tag for Gesture Recognition," *IEEE Sensors J.*, vol. 21, no. 16, pp. 18 279–18 286, 2021.
- [10] E. Perret, *Radio Frequency Identification and Sensors: From RFID to Chipless RFID*. Hoboken, NJ, USA: Wiley: Wiley, 2014.
- [11] Nemai Chandra Karmakar, Emran Md Amin, and Jhantu Kumar Saha, *Chipless RFID Sensors*. John Wiley & Sons, Inc, Jan. 2016.
- [12] Z. Ali *et al.*, "Authentication Using Metallic Inkjet-Printed Chipless RFID Tags," *IEEE Trans. Antennas Propag.*, vol. 68, no. 5, pp. 4137–4142, 2020.
- [13] N. Barbot and E. Perret, "Accurate Positioning System Based on Chipless Technology," *Sensors*, vol. 19, no. 6, 2019.
- [14] M. A. Herráez, D. R. Burton, M. J. Lalor, and M. A. Gdeisat, "Fast two-dimensional phase-unwrapping algorithm based on sorting by reliability following a noncontinuous path," *Applied Optics*, vol. 41, no. 35, pp. 7437–7444, Dec 2002.
- [15] O. Rance, E. Perret, R. Siragusa, and P. Lemaitre-Auger, *RCS Synthesis for Chipless RFID: Theory and Design*. Elsevier, 2017.
- [16] Z. Ali, N. Barbot, and E. Perret, "Demonstration of Gesture Recognition Using Chipless RFID Tag Held in Hand." [Online]. Available: <https://youtu.be/12TSYr6cx10>